

Generation and stabilization of entangled coherent states for the vibrational modes of a trapped ion

Zhi-Rong Zhong,¹ Xin-Jie Huang,¹ Zhen-Biao Yang,¹ Li-Tuo Shen,¹ and Shi-Biao Zheng^{1,*}

¹*Fujian Key Laboratory of Quantum Information and Quantum Optics, College of Physics and Information Engineering, Fuzhou University, Fuzhou, Fujian 350116, China*

(Dated: May 14, 2019)

We propose a scheme for preparation of entangled coherent states for the motion of an ion in a two-dimensional anisotropic trap. In the scheme, the ion is driven by four laser beams along different directions in the ion trap plane, resulting in carrier excitation and couplings between the internal and external degrees of freedom. When the total quantum number of the vibrational modes initially has a definite parity, the competition between the unitary dynamics and spontaneous emission will force the system to evolve to a steady state, where the vibrational modes are in a two-mode cat state. We show that the method can be extended to realization of entangled coherent states for three vibrational modes of an ion in three-dimensional anisotropic trap.

PACS numbers: 42.50.Vk, 42.50.Dv.

I. INTRODUCTION

The superposition principle, distinguishing between the quantum and classical worlds, lies at the heart of quantum mechanics. Superimposing two state components gives rise to new nonclassical effects due to the quantum interference between these components. This is well exemplified by superpositions of macroscopically distinguishable states, known as Schrodinger cat states [1]. In quantum optics, cat states are defined as superpositions of two distinct quantum states closest to classical ones—coherent states with different phases or amplitudes. Though formed by quasiclassical states, cat states can exhibit strongly nonclassical behaviors, i.e., negativity of the quasiprobability distribution in phase space [2]. These superposition states are central to exploration of the fuzzy quantum-classical boundary, and useful for redundant encoding required for quantum error correction [3-6]. Such states have been experimentally generated in various systems, including cavity quantum electrodynamics (QED) [2,7], superconducting circuits [8-13], and ion traps [14-16].

The application of the superposition principle to composite systems will give rise to a more striking quantum phenomenon, i.e., entanglement, originally introduced by Einstein et al. to question the completeness of quantum mechanics. Among various entangled states, entangled coherent states of two harmonic oscillators [17], also referred to as two-mode cat states [18], are strikingly interesting. The entanglement between quasiclassical state components leads to interesting nonclassical properties, such as two-mode squeezing, violations of Cauchy-Schwartz inequality, quantum interference features in four-dimensional phase space, and violations of Bell inequalities. Apart from fundamental interest, these

entangled states have practical applications in quantum information processing [19] and quantum metrology [20]. Schemes have been proposed for producing such states for two mesoscopic fields through reservoir engineering in cavity QED [21,22] and circuit QED [23]. Recently, these states have been produced in a circuit [24], where the microwave fields stored in two three-dimensional cavities were entangled by dispersively coupling them to a superconducting qubit.

Ion traps represent another qualified candidate for quantum state engineering and quantum information processing. The prominent properties of this system is that the damping of the vibrational modes is extremely weak, and these bosonic modes can be controllably coupled to the electronic state via laser driving. In addition to the Schrodinger cat states [14-16], squeezed states [25], Fock states [25], and superpositions of Fock states [26] have been experimentally produced for one vibrational mode of a trapped ion. Entanglement consisting of zero- and one-phonon states has also been observed for two vibrational modes, each belonging to one pair of trapped ions [27]. On the other hand, proposals have been suggested for generating various entangled states for two vibrational degrees of freedom of a trapped ion, including pair coherent states [28], superpositions of pair coherent states [29], SU(1,1) intelligent states [30], two-mode squeezed pair coherent states [31], entangled coherent states [32,33], and arbitrary superpositions of two-mode Fock states [34-38]. The schemes proposed in Refs. [32] and [33] are relying on measurement of the ionic internal state to conditionally project the vibrations to the desired state after suitable laser driving, while those of Refs. [34], [35], [36], [37], and [38] allow for deterministic generation of arbitrary entangled states in the Fock state basis through step-by-step procedures, following which any entangled coherent state can be approximately realized by approaching its Fock state expansion, with the number of required operations increasing with the average quantum number of each mode. We here propose

* t96034@fzu.edu.cn

an unconditional scheme for generating such states of the two vibrational modes of an ion confined in a two-dimensional anisotropic harmonic trap. In our scheme, the ion is driven by four lasers of different frequencies on the xy plane. With suitable setting of the parameters and directions of these lasers, the system steady state is given by the product of the electronic ground state with a vibrational two-mode cat state if the two vibrational modes initially have a definite joint parity. Unlike the previous schemes [32-38], our scheme requires neither the projective measurement of the ionic electronic state nor a sequence of operations achieved by frequently tuning the parameters of the driving laser. Another distinct feature of our scheme is that it not only allows for the generation of entangled coherent states, but also can be used to stabilize these states.

The paper is organized as follows. In Sec. 2, we present the theoretical model, in which the internal state of a trapped ion is coupled to its vibrational modes along two mutually perpendicular directions by laser driving. The unitary dynamics associated with this coupling, together with the decaying of the internal state, forces the system to evolve to the steady state, where the two vibrational modes are in a two-mode cat state. In Sec 3, we present numerical simulations of the fidelities of the vibrational states to the desired cat states with the dissipation of the vibrational modes being included, confirming the validity of our scheme. We also display the Wigner functions of the vibrational modes in the steady state, which show good agreement with the ideal cat states. In Sec. 4, we show that the scheme can be generalized to drive three vibrational modes of an ion confined in an anisotropic three-dimensional harmonic trap into a three-mode cat state. A summary appears in Sec. 5.

II. THEORETICAL MODEL

We consider an ion trapped in an anisotropic harmonic potential, with the vibrational frequencies along the x

and y axes are ν_x and ν_y , respectively. The transition between the electronic ground state $|g\rangle$ and one excited state $|e\rangle$ are driven by four laser beams of frequencies $\omega_0 - 2\omega_x$, $\omega_0 - 2\omega_y$, $\omega_0 - \omega_x - \omega_y$, and ω_0 , where ω_0 is the transition frequency between $|g\rangle$ and $|e\rangle$. The first two are aligned along the x and y axes, while the other two are at angles of $\pi/4$ and $-\pi/4$ to x axis, respectively. In the rotating-wave approximation, the Hamiltonian for this system is given by (setting $\hbar = 1$)

$$H = \omega_x a^\dagger a + \omega_y b^\dagger b + \omega_0 S_z + [\lambda E^+(x, y, t) S^+ + H.c.], \quad (1)$$

where a^\dagger (b^\dagger) and a (b) are the creation and annihilation operators for the vibrational modes along the x and y axes and of frequencies ω_x and ω_y , respectively, S^+ , S^- , and S_z are the raising, lowering, and inversion operators for the electronic dipole transition, and λ is the transition frequency and dipole matrix element. $E^+(x, t)$ is the positive part of the classical driving fields

$$\begin{aligned} E^+(x, t) = & E_1 e^{-i[(\omega_0 - 2\omega_x)t - k_1 x + \phi_1]} \\ & + E_2 e^{-i[(\omega_0 - 2\omega_y)t - k_2 y + \phi_2]} \\ & + E_3 e^{-i[(\omega_0 - \omega_x - \omega_y)t - k_3(x+y)/\sqrt{2} + \phi_3]} \\ & + E_0 e^{-i[\omega_0 t - k_0(x-y)/\sqrt{2} + \phi_0]}, \end{aligned} \quad (2)$$

where E_n , ϕ_n , and k_n ($n = 0, 1, 2, 3$) are the amplitudes, phases, and wave vectors of the n th driving field, respectively. The position operators x and y can be expressed by $x = \sqrt{1/(2\omega_x M)}(a + a^\dagger)$ and $y = \sqrt{1/(2\omega_y M)}(b + b^\dagger)$, with M being the mass of the trapped ion.

In the resolved sideband limit the vibrational frequencies ω_x and ω_y are much larger than other characteristic frequencies of the problem. Then the interactions of the ion with lasers can be treated using nonlinear Jaynes-Cummings model [39]. In this case the Hamiltonian for such a system, in the interaction picture, is given by

$$\begin{aligned} H_i = & \sum_{j=0}^{\infty} \left\{ e^{-\eta_x^2/2} \frac{(i\eta_x)^{2j+2}}{j!(j+2)!} \Omega_1 e^{-i\phi_1} a^{\dagger j} a^{j+2} + e^{-\eta_y^2/2} \frac{(i\eta_y)^{2j+2}}{j!(j+2)!} \Omega_2 e^{-i\phi_2} b^{\dagger j} b^{j+2} + \sum_{l=0}^{\infty} e^{-(\eta_x^2 + \eta_y^2)/4} \right. \\ & \left. \left[\frac{(i\eta_x/\sqrt{2})^{2j+1}}{j!(j+1)!} \frac{(i\eta_y/\sqrt{2})^{2l+1}}{l!(l+1)!} \Omega_3 e^{-i\phi_3} a^{\dagger j} a^{j+1} b^{\dagger l} b^{l+1} + \frac{(i\eta_x/\sqrt{2})^{2j}}{(j!)^2} \frac{(-i\eta_y/\sqrt{2})^{2l}}{(l!)^2} \Omega_0 e^{-i\phi_0} a^{\dagger j} a^j b^{\dagger l} b^{l+1} \right] \right\} S^+ \\ & + H.c., \end{aligned} \quad (3)$$

where $\Omega_n = \lambda E_n$ are the Rabi frequencies of the respective lasers, and $\eta_x = k_0/\sqrt{2\omega_x M}$ and $\eta_y = k_0/\sqrt{2\omega_y M}$ are the Lamb-Dicke parameters associated with the vibrational modes along the x and y axes, respectively. We here set $k_1 \simeq k_2 \simeq k_3 \simeq k_0$.

We consider the behavior of the ion in the Lamb-Dicke regime, $\eta_x, \eta_y \ll 1$. In this limit we can discard the terms with $j > 0$ or $l > 0$. Then the Hamiltonian can be

simplified to

$$H_i = \left[-\frac{\eta_x^2}{2} e^{-\eta_x^2/2} \Omega_1 e^{-i\phi_1} a^2 - \frac{\eta_y^2}{2} e^{-\eta_y^2/2} \Omega_2 e^{-i\phi_2} b^2 + e^{-(\eta_x^2 + \eta_y^2)/4} \left(-\frac{\eta_x \eta_y}{2} \Omega_3 e^{-i\phi_3} ab + \Omega_0 e^{-i\phi_0} \right) \right] S^+ + H.c., \quad (4)$$

The phase difference $\phi_n - \phi_m$ is equal to the relative phase between the n th and m th driving fields, and the ratio between the Rabi frequencies Ω_n and Ω_m depends on the ratio between the amplitudes of these two fields. Therefore, we can choose the relative phases and amplitudes of the lasers appropriately so that

$$\begin{aligned} \phi_1 &= \phi_2 = \phi_3 = \phi_0, \\ \eta_x^2 e^{-\eta_x^2/2} \Omega_1 &= \eta_y^2 e^{-\eta_y^2/2} \Omega_2 = \frac{\eta_x \eta_y}{2} e^{-(\eta_x^2 + \eta_y^2)/4} \Omega_3 = 2\lambda, \end{aligned} \quad (5)$$

Then we obtain

$$H_i = [-\lambda(a+b)^2 + \varepsilon] e^{-i\phi_0} S^+ + H.c. \quad (6)$$

where

$$\varepsilon = e^{-(\eta_x^2 + \eta_y^2)/4} \Omega_0. \quad (7)$$

The evolution of the vibrational modes is independent of the phase factor $e^{-i\phi_0}$ in Eq. (6), which can be set to be 1 in the calculation of the motional state.

The damping of the vibrational modes is so weak that it can be disregarded and thus the electronic damping is the main decaying process [28-31,40,41]. Then the evolution of the whole system is described by the master equation for the master operator ρ

$$\frac{d\rho}{dt} = -i[H_i, \rho] + \frac{\Gamma}{2} (2S^- \rho S^+ - S^+ S^- \rho - \rho S^+ S^-), \quad (8)$$

where Γ is the spontaneous decay rate of the excited state of the ion. In the long time limit, the system will reach the steady state, satisfying

$$\frac{d\rho_s}{dt} = 0. \quad (9)$$

In the steady state, the ion will be populated in the ground electronic state $|g\rangle$ due to the spontaneous emission. As a consequence, the steady state solution of the master equation (15) can be rewritten as

$$\rho_s = |g\rangle \langle g| \otimes |\psi\rangle \langle \psi|, \quad (10)$$

where $|\psi\rangle$ stands for the correlated state of the motions in the x and y axes. Since the dissipative term has no effect on the electronic ground state, the condition for the system to reach the steady state is $[H_i, \rho_s] = 0$. This leads to

$$\lambda(a+b)^2 |\psi\rangle = \varepsilon |\psi\rangle. \quad (11)$$

Any combination of the two-mode coherent states $|\alpha_1\rangle_a |\alpha_2\rangle_b$ and $|-\alpha_1\rangle_a |-\alpha_2\rangle_b$ satisfies this equation, where $|\alpha_1\rangle_a$ and $|\alpha_2\rangle_b$ are the coherent states for the vibrational modes along the x and y axes, respectively, with $\alpha_1 + \alpha_2 = \sqrt{\varepsilon/\lambda}$. The values of α_1 and α_2 depend on the initial state of the vibrational modes. When they are initially in an eigenstate of the parity operator $\Pi = (-1)^{(a^\dagger + b^\dagger)(a+b)}$, the two modes remain symmetric during the evolution and the two-mode state components in the steady state are $|\alpha\rangle_a |\alpha\rangle_b$ and $|-\alpha\rangle_a |-\alpha\rangle_b$, with $\alpha = \frac{1}{2}\sqrt{\varepsilon/\lambda}$. We note the operator Π commutes with the system Hamiltonian, so that the parity is conserved during the process. When the parity is initially even, the vibrational modes will finally evolve to the even two-mode cat state

$$|\psi_+\rangle = \mathcal{N}_+ (|\alpha\rangle_a |\alpha\rangle_b + |-\alpha\rangle_a |-\alpha\rangle_b), \quad (12)$$

where $\mathcal{N}_+ = (2 + 2e^{-4|\alpha|^2})^{-1/2}$. On the other hand, for the odd parity, the steady state corresponds to the two-mode odd cat state

$$|\psi_-\rangle = \mathcal{N}_- (|\alpha\rangle_a |\alpha\rangle_b - |-\alpha\rangle_a |-\alpha\rangle_b), \quad (13)$$

where $\mathcal{N}_- = (2 - 2e^{-4|\alpha|^2})^{-1/2}$. We note that the system steady state remains unchanged when the dephasing of the electronic degree of freedom is included in the master equation. This is due to the fact that this degree of freedom is finally in the ground state and not affected by dephasing.

III. NUMERICAL SIMULATIONS

To verify the validity of the proposed scheme, we perform a numerical simulation of the fidelity of the system steady state with respect to the target state. We first suppose that the target state is an even two-mode cat state $|\psi_+\rangle$ with $\alpha = 2$. To generate such a state, we assume that the two vibrational modes are initially in the vacuum state $|0\rangle_a |0\rangle_b$, and the internal degree of freedom is initially in the ground state $|g\rangle$. With the coupling between the vibrational modes and the reservoir being included, the master equation is

$$\begin{aligned} \frac{d\rho}{dt} &= -i[H_i, \rho] + \frac{\Gamma}{2} (2S^- \rho S^+ - S^+ S^- \rho - \rho S^+ S^-) \\ &\quad + \frac{\gamma_a}{2} (2a\rho a^\dagger - a^\dagger a \rho - \rho a^\dagger a) \\ &\quad + \frac{\gamma_b}{2} (2b\rho b^\dagger - b^\dagger b \rho - \rho b^\dagger b), \end{aligned} \quad (14)$$

where γ_a and γ_b are the decaying rates of the two vibrational modes, respectively. We set $\eta_x = 0.15$, $\eta_y = 0.1$, $\varepsilon = 16\lambda$, $\Gamma = 100\lambda$, and $\gamma_a = \gamma_b = 0.0005\lambda$. To verify the validity of the Lamb-Dicke approximation, here we retain the dominant higher-order terms ($j + l = 1$) in

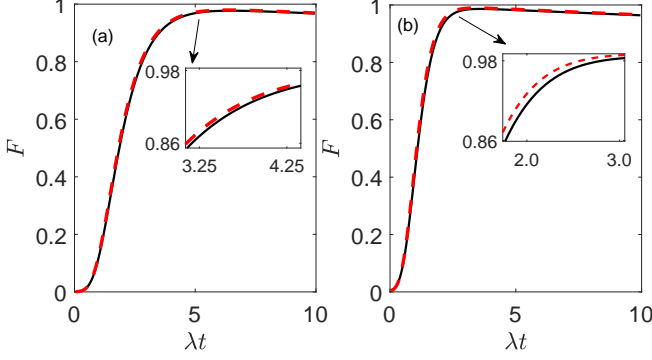


FIG. 1. (Color online) (a) Fidelity of the generated vibrational state to the expected state as a function of λt with the initial state $|g\rangle|0\rangle_a|0\rangle_b$. The generated vibrational state is calculated by numerically solving Eq. (14), with the parameters $\eta_x = 0.15$, $\eta_y = 0.1$, $\varepsilon = 16\lambda$, $\Gamma = 100\lambda$, and $\gamma_a = \gamma_b = 0.0005\lambda$. The corresponding expected state is $\mathcal{N}_+(|\alpha\rangle_a|\alpha\rangle_b + |-\alpha\rangle_a|-\alpha\rangle_b)$ with $\alpha = 2$. The black-solid and red-dashed lines represent the results with and without consideration of the dominant higher-order terms of the Hamiltonian, respectively. (b) Fidelity of the generated vibrational state to the expected state as a function of λt with the initial state $|g\rangle(|1\rangle_a|0\rangle_b + |0\rangle_a|1\rangle_b)/\sqrt{2}$. The corresponding expected state is $\mathcal{N}_-(|\alpha\rangle_a|\alpha\rangle_b - |-\alpha\rangle_a|-\alpha\rangle_b)$ with $\alpha = 2$. The unit of this figure is λ .

Eq (3), so that the Hamiltonian is

$$H_i = \left[-\lambda \left(1 - \frac{\eta_x^2}{3} a^\dagger a \right) a^2 - \lambda \left(1 - \frac{\eta_y^2}{3} b^\dagger b \right) b^2 - 2\lambda \left(1 - \frac{\eta_x^2}{4} a^\dagger a - \frac{\eta_y^2}{4} b^\dagger b \right) ab + \varepsilon \left(1 - \frac{\eta_x^2}{2} a^\dagger a - \frac{\eta_y^2}{2} b^\dagger b \right) \right] e^{-i\phi_0} S^+ + H.c., \quad (15)$$

Fig. 1(a) shows the fidelity (black-solid line), defined as $F = \langle \psi_+ | \rho_{a,b} | \psi_+ \rangle$, as a function of the evolution time, where $\rho_{a,b}$ is the reduced density operator of the two vibrational modes, obtained by tracing the total system density operator over the internal degree of freedom. The numerical result shows that the system approaches the steady state when $\lambda t \simeq 6.5$; at this time the fidelity is $F \simeq 0.977$. In Fig. 1(b), we display numerical simulation of the evolution of the fidelity for the obtained vibrational state to the ideal odd cat state $|\psi_-\rangle$ with the initial state $|g\rangle(|1\rangle_a|0\rangle_b + |0\rangle_a|1\rangle_b)/\sqrt{2}$, where $|1\rangle_a$ and $|1\rangle_b$ denote the one-phonon Fock state for modes a and b, respectively. In this case the corresponding fidelity is about $F \simeq 0.986$ at the time $\lambda t \simeq 3.5$. Compared to the cases without taking the higher-order terms into consideration (red-dashed lines), the steady state fidelities are decreased by only about 0.25%, confirming the validity

of the approximation.

To further demonstrate the production of the desired entanglement in each steady state, we calculate the corresponding joint Wigner function of the two bosonic modes, defined as the joint quasiprobability distribution for these modes in four-dimensional phase space

$$W(\beta, \chi) = \frac{4}{\pi^2} \left\langle D_a(\beta) (-1)^{a^\dagger a} D_a^\dagger(\beta) D_b(\chi) (-1)^{b^\dagger b} D_b^\dagger(\chi) \right\rangle, \quad (16)$$

where $D_a(\beta) = e^{\beta a^\dagger - \beta^* a}$ and $D_b(\chi) = e^{\chi b^\dagger - \chi^* b}$ are displacement operators for the vibrational modes along the x and y axes, respectively, with β and χ being complex parameters, which define the coordinates in the joint phase space [24]. The dominant higher-order terms in the Hamiltonian are included in the calculation of $W(\beta, \chi)$. The plane-cut of the Wigner function along the $\text{Im}(\beta)$ - $\text{Im}(\chi)$ axes for the ideal even two-mode cat state with $\alpha = 2$ is shown in Fig. 2 (a), while that for the steady state obtained with the initial state $|g\rangle|0\rangle_a|0\rangle_b$ and the above mentioned parameters at the time $\lambda t = 7$ is shown in Fig. 2 (b). The fringes with alternating positive and negative values on the $\text{Im}(\beta)$ - $\text{Im}(\chi)$ plane-cut are the signatures of quantum interference between the two quasi-classical components. The plane-cuts of the Wigner functions along the $\text{Im}(\beta)$ - $\text{Im}(\chi)$ axes for the ideal odd two-mode cat state with $\alpha = 2$ and for the steady state obtained with the initial state $|g\rangle(|1\rangle_a|0\rangle_b + |0\rangle_a|1\rangle_b)/\sqrt{2}$ at the time $\lambda t = 4$ are shown in Fig. 3 (a) and (b), respectively. As expected, for each initial state the plane-cuts of the Wigner function along the $\text{Im}(\beta)$ - $\text{Im}(\chi)$ axes obtained from the steady state is in well agreement with the result for the ideal cat state, and the interference features associated with the two initial states are complementary.

IV. GENERATION OF THREE-MODE CAT STATES

We now turn to the case that the ion is in a three-dimensional anisotropic trap, with the vibrational frequencies along the x, y, and z axes being ω_x , ω_y , and ω_z , respectively. The ion is driven by six laser beams of frequencies $\omega_0 - 2\omega_x$, $\omega_0 - 2\omega_y$, $\omega_0 - 2\omega_z$, $\omega_0 - \omega_x - \omega_y$, $\omega_0 - \omega_y - \omega_z$, $\omega_0 - \omega_x - \omega_z$, and ω_0 . The first three laser beams are aligned along the x and y axes, the fourth is on the x-y plane and at angle of $\pi/4$ to x axis, the fifth is on the y-z plane and at an angle of $\pi/4$ to y axis, the sixth is on the x-z plane and at angle of $\pi/4$ to x axis, and the last one is on the x-y plane and at an angle of $-\pi/4$ to x axis. In the rotating-wave approximation, the Hamiltonian for this system is given by

$$E^+(x, t) = E_1 e^{-i[(\omega_0 - 2\omega_x)t - k_1 x]} + E_2 e^{-i[(\omega_0 - 2\omega_y)t - k_2 y]} + E_3 e^{-i[(\omega_0 - 2\omega_y)t - k_3 z]} + E_4 e^{-i[(\omega_0 - \omega_x - \omega_y)t - k_4(x+y)/\sqrt{2}]} + E_5 e^{-i[(\omega_0 - \omega_y - \omega_z)t - k_5(y+z)/\sqrt{2}]} + E_6 e^{-i[(\omega_0 - \omega_x - \omega_z)t - k_6(x+z)/\sqrt{2}]} + E_0 e^{-i[\omega_0 t - k_0(x-y)/\sqrt{2}]} \quad (17)$$

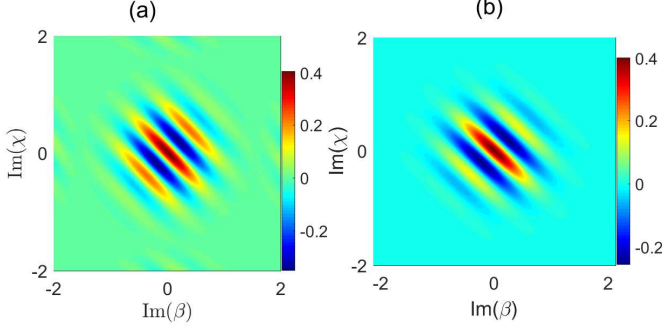


FIG. 2. (Color online) (a) Plane-cut of the two-mode Wigner function $W(\beta, \chi)$ along the $\text{Im}(\beta)$ - $\text{Im}(\chi)$ axes for the ideal cat state $\mathcal{N}_+(|\alpha\rangle_a |\alpha\rangle_b + |-\alpha\rangle_a |-\alpha\rangle_b)$ with $\alpha = 2$. (b) Plane-cut of $W(\beta, \chi)$ along the $\text{Im}(\beta)$ - $\text{Im}(\chi)$ axes obtained by numerically solving Eq. (8) with the initial state $|g\rangle |0\rangle_a |0\rangle_b$. The parameters are the same as those in Fig. 1, and the dominant higher-order terms in the Hamiltonian are included. The unit of this figure is λ .

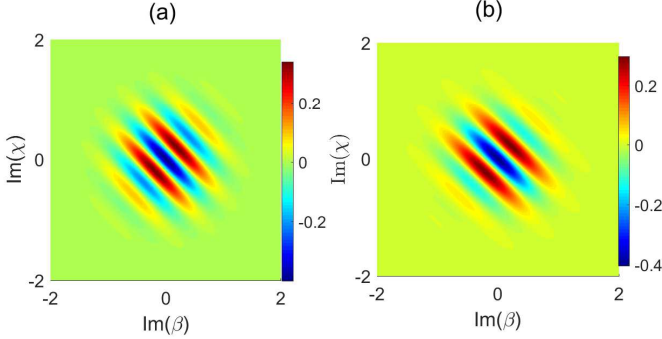


FIG. 3. (Color online) (a) Plane-cut of $W(\beta, \chi)$ along the $\text{Im}(\beta)$ - $\text{Im}(\chi)$ axes for the ideal cat state $\mathcal{N}_-(|\alpha\rangle_a |\alpha\rangle_b - |-\alpha\rangle_a |-\alpha\rangle_b)$ with $\alpha = 2$. (b) Plane-cut of $W(\beta, \chi)$ along the $\text{Im}(\beta)$ - $\text{Im}(\chi)$ axes for the vibrational modes obtained by simulating the master equation with the initial state $|g\rangle (|1\rangle_a |0\rangle_b + |0\rangle_a |1\rangle_b) / \sqrt{2}$. The parameters are the same as those in Fig. 1, and the dominant higher-order terms in the Hamiltonian are included. The unit of this figure is λ .

We here have assumed that the phase for each laser beam is 0. In the resolved sideband limit and in the Lamb-Dicke regime, the effective Hamiltonian for the system

is

$$H_i = \left[\frac{-\eta_x^2}{2} e^{-\eta_x^2/2} \Omega_1 a^2 - \frac{\eta_y^2}{2} e^{-\eta_y^2/2} \Omega_2 b^2 - \frac{\eta_z^2}{2} e^{-\eta_z^2/2} \Omega_3 c^2 - \frac{\eta_x \eta_y}{2} e^{-(\eta_x^2 + \eta_y^2)/4} \Omega_4 ab - \frac{\eta_y \eta_z}{2} e^{-(\eta_y^2 + \eta_z^2)/4} \Omega_5 bc - \frac{\eta_x \eta_z}{2} e^{-(\eta_x^2 + \eta_z^2)/4} \Omega_6 ac + e^{-(\eta_x^2 + \eta_y^2)/4} \Omega_0 \right] S^+ + H.c., \quad (18)$$

where c is the annihilation operator for the vibrational mode along the z axis. We choose the amplitudes of the lasers appropriately so that

$$\begin{aligned} \eta_x^2 e^{-\eta_x^2/2} \Omega_1 &= \eta_y^2 e^{-\eta_y^2/2} \Omega_2 = \eta_z^2 e^{-\eta_z^2/2} \Omega_3 = \lambda, \\ \eta_x \eta_y e^{-(\eta_x^2 + \eta_y^2)/4} \Omega_4 &= \eta_y \eta_z e^{-(\eta_y^2 + \eta_z^2)/4} \Omega_5 \\ &= \eta_x \eta_z e^{-(\eta_x^2 + \eta_z^2)/4} \Omega_6 = 2\lambda, \end{aligned} \quad (19)$$

then we obtain

$$H_i = [-\lambda(a + b + c)^2 + \varepsilon] S^+ + H.c. \quad (20)$$

When the decaying of the electronic state is included, the system dynamics is governed by the master equation of form of Eq. (8). The system steady state is again of the form of Eq. (10), where $|\psi\rangle$ satisfies

$$\lambda(a + b + c)^2 |\psi\rangle = \varepsilon |\psi\rangle. \quad (21)$$

When the vibrational modes are initially in an eigenstate of the parity operator $\Pi = (-1)^{(a^\dagger + b^\dagger + c^\dagger)(a + b + c)}$, $|\psi\rangle$ is a superposition of $|\alpha\rangle_a |\alpha\rangle_b |\alpha\rangle_c$ and $|-\alpha\rangle_a |-\alpha\rangle_b |-\alpha\rangle_c$, with $\alpha = \frac{1}{3} \sqrt{\varepsilon/\lambda}$. The relative superposition coefficient of the two components in the steady state depends on the initial parity. When these modes are initially in the vacuum state $|0\rangle_a |0\rangle_b |0\rangle_c$, they will finally evolve to the even three-mode cat state

$$|\psi_+\rangle = \mathcal{N}_+ (|\alpha\rangle_a |\alpha\rangle_b |\alpha\rangle_c + |-\alpha\rangle_a |-\alpha\rangle_b |-\alpha\rangle_c), \quad (22)$$

where $\mathcal{N}_+ = (2 + 2e^{-8|\alpha|^2})^{-1/2}$. On the other hand, if the vibrational modes are initially in the state $(|1\rangle_a |0\rangle_b |0\rangle_c + |0\rangle_a |1\rangle_b |0\rangle_c + |0\rangle_a |0\rangle_b |1\rangle_c) / \sqrt{3}$, the steady state corresponds to the three-mode odd cat state

$$|\psi_-\rangle = \mathcal{N}_- (|\alpha\rangle_a |\alpha\rangle_b |\alpha\rangle_c - |-\alpha\rangle_a |-\alpha\rangle_b |-\alpha\rangle_c), \quad (23)$$

where $\mathcal{N}_- = (2 - 2e^{-8|\alpha|^2})^{-1/2}$.

V. SUMMARY

In conclusion, we have proposed a scheme for producing entangled coherent states of the vibrational modes

of an ion trapped in a two-dimensional anisotropic harmonic well. In our scheme, the ion is driven by four laser beams, one of which is used to directly coupling the two electronic states, while the others serve for coupling the electronic transition with the vibrational modes. In the Lamb-Dicke limit and with appropriate setting of the laser parameters, the combination of the unitary dynamics and spontaneous emission will evolve the system to a steady state, given by the product of the electronic ground state with a two-mode vibrational state. When the two vibrational modes are initially in a Fock state, their steady state corresponds to a cat state. Numerical simulations confirm the validity of the proposed scheme.

We further show that the method can be generalized to realization of three-mode cat states for an ion trapped in a two-dimensional anisotropic harmonic well. We note the idea may also be applied to generation and stabilization of entangled coherent states for two cavity modes by coupling them to an atom or an artificial atom.

This work was supported by the National Natural Science Foundation of China under Grant No. 11674060 and No. 11705030, the Natural Science Foundation of Fujian Province under Grant No. 2016J01018, and the Fujian Provincial Department of Education under Grant No. JZ160422.

-
- [1] E. Schrödinger, *Naturwissenschaften* 23, 807 (1935).
 [2] S. Deléglise, I. Dotsenko, C. Sayrin, J. Bernu, M. Brune, J.-M. Raimond, and S. Haroche, *Nature* 455, 510 (2008).
 [3] Z. Leghtas et al., *Phys. Rev. Lett.* 111, 120501 (2013).
 [4] M. Mirrahimi et al., *New J. Phys.* 16, 045014 (2014).
 [5] N. Ofek et al., *Nature (London)* 536, 441 (2016).
 [6] V. V. Albert et al., *Phys. Rev. Lett.* 116, 140502 (2016).
 [7] M. Brune et al., *Phys. Rev. Lett.* 77, 4887 (1996).
 [8] M. Hofheinz et al., *Nature (London)* 459, 546 (2009).
 [9] S.-B. Zheng et al., *Phys. Rev. Lett.* 115, 260403 (2015).
 [10] B. Vlastakis, G. Kirchmair, Z. Leghtas, S. E. Nigg, L. Frunzio, S. M. Girvin, M. Mirrahimi, M. H. Devoret, and R. J. Schoelkopf, *Science* 342, 607 (2013).
 [11] L. Sun et al., *Nature* 511, 444C448 (2014).
 [12] B. Vlastakis et al., *Nat. Commun.* 6, 8970 (2015).
 [13] K. Liu et al., *Sci. Adv.* 3, e1603159 (2017).
 [14] C. Monroe, D. M. Meekhof, B. E. King and D. J. Wineland, *Science* 272, 1131 (1996).
 [15] C. Hempel et al., *Nat. Photonics* 7, 630 (2013).
 [16] K. G. Johnson, J. D. Wong-Campos, B. Neyenhuis, J. Mizrahi, and C. Monroe, *Nature Communications* 8, 697 (2017).
 [17] B. C. Sanders, *Phys. Rev. A* 45, 6811 (1992).
 [18] C. Chai, *Phys. Rev. A* 46, 7187 (1992).
 [19] B. C. Sanders, *J. Phys. A: Math. Theor.* 45, 244002 (2012).
 [20] J. Joo, W. J. Munro, and T. P. Spiller, *Phys. Rev. Lett.* 107, 083601 (2011).
 [21] A. Sarlette, Z. Leghtas, M. Brune, J. M. Raimond, and P. Rouchon, *Phys. Rev. A* 86, 012114 (2012).
 [22] C. Arenz, C. Cormick, D. Vitali, and G. Morigi, *J. Phys. B: At. Mol. Opt. Phys.* 46, 224001 (2013).
 [23] M. Mamaev, L. C. G. Govia, and A. A. Clerk, [arXiv:1711.06662](https://arxiv.org/abs/1711.06662).
 [24] C. Wang et al., *Science* 352, 1087 (2016).
 [25] D. M. Meekhof, C. Monroe, B. E. King, W. M. Itano, and D. J. Wineland, *Phys. Rev. Lett.* 76, 1796 (1996).
 [26] B. DeMarco, A. Ben-Kish, D. Leibfried, V. Meyer, M. Rowe, B.M. Jelenković, W.M. Itano, J. Britton, C. Langer, T. Rosenband, and D.J. Wineland, *Phys. Rev. Lett.* 90, 037902 (2003).
 [27] J. D. Jost, J. P. Home, J. M. Amini, D. Hanneke, R. Ozeri, C. Langer, J. J. Bollinger, D. Leibfried, and D. J. Wineland, *Nature* 459, 683 (2009).
 [28] S. -C. Gou, J. Steinbach and P. L. Knight, *Phys. Rev. A* 54, R1014 (1996).
 [29] S. -C. Gou, J. Steinbach and P. L. Knight, *Phys. Rev. A* 54, 4315 (1996).
 [30] C. C. Gerry, S. -C. Gou and J. Steinbach, *Phys. Rev. A* 55, 630 (1997).
 [31] S. -B. Zheng and G. -C. Guo, *Quantum Semiclass. Opt.* 10, 441 (1998).
 [32] S. -B. Zheng, *Phys. Rev. A* 58, 761 (1998).
 [33] C. C. Gerry, *Phys. Rev. A* 55, 2478 (1997).
 [34] S. A. Gardiner, J. I. Cirac, and P. Zoller, *Phys. Rev. A* 55, 1683 (1997).
 [35] B. Kneer and C. K. Law, *Phys. Rev. A* 57, 2096 (1998).
 [36] G. Drobny, B. Hladky, and V. Buzek, *Phys. Rev. A* 58, 2481 (1998).
 [37] S.-B. Zheng, *Phys. Rev. A* 63, 015801 (2001).
 [38] X.-B Zou, K Pahlke, and W Mathis, *Phys. Rev. A* 65, 045801 (2002).
 [39] W. Vogel and R. L. de Matos Filho, *Phys. Rev. A* 52, 4214 (1995).
 [40] R. L. de Matos Filho and W. Vogel, *Phys. Rev. Lett.* 76, 608 (1996).
 [41] N. B. An and T. M. Duc, *Phys. Rev. A* 66, 065401 (2002).